Transportation Research Part D 149 (2025) 105063

Contents lists available at ScienceDirect

Transportation Research Part D

journal homepage: www.elsevier.com/locate/trd

# National road traffic noise estimation with ensemble learning and multimodal geodata

Jeroen Staab [a,b,*], Matthias Weigand [a,c], Arthur Schady [d], Ariane Droin [a,c], Donatella Cea [e], Marco Dallavalle [f,g], Nikolaos Nikolaou [f], Mahyar Valizadeh [e], Kathrin Wolf [f], Michael Wurm [a], Tobia Lakes [b], Hannes Taubenböck [a,c]

[a] German Remote Sensing Data Center, Department for Geo-Risks and Civil Security, German Aerospace Center (DLR), Oberpfaffenhofen, Germany
[b] Geography Department, Humboldt-Universität zu Berlin, Berlin, Germany
[c] Institute for Geography and Geology, Julius-Maximilians-Universität Würzburg, Würzburg, Germany
[d] Institute of Atmospheric Physics, Applied Meteorology Department, German Aerospace Center (DLR), Oberpfaffenhofen, 82234, Germany
[e] Helmholtz AI, Helmholtz Munich, German Research Center for Environmental Health, Neuherberg, Germany
[f] Institute of Epidemiology, Helmholtz Munich, German Research Center for Environmental Health, Neuherberg, Germany
[g] Institute for Medical Information Processing, Biometry and Epidemiology (IBE), Faculty of Medicine, LMU Munich, Pettenkofer School of Public Health, Munich, Germany

ARTICLE INFO

*Keywords:*
Noise pollution
Road traffic noise
Random forest
Ensemble learning
Multimodal geodata
Noise exposure
Urban noise mapping
Environmental health

ABSTRACT

The European Noise Directive mandates the mapping of noise – high, continuous sound pressure levels considered to be a major health threat. However, the strictest rulesets apply to specific regions only and the majority of residential areas are unmapped. Transfer learning was deployed to close spatial data gaps between the official, strategic road traffic noise maps. The three most suitable hyperparameter configurations achieved weighted Kappa values (a measure of ordinal agreement) ranging between 0.889 and 0.956 during repeated cross-validation. The best model achieved an overall classification accuracy of 90.7 % when tested against held-out samples. 7.8 % of predictions exhibited minor deviations within ± 5 dB(A). The model was subsequently deployed to predict road traffic noise across Germany at 10 x 10 Meter resolution for 2017. The results suggest a total of 13.1 million people exposed to yearly averaged road traffic noise ($L_{den}$) above 55 dB(A) and stress need for improved noise policies.

## 1. Introduction

Loud and stressful noise poses a major threat to human health (Basner et al., 2014; Stansfeld, 2003; World Health Organization, 2011), animals (Brumm, 2013) and the natural environment in general (Francis et al., 2012). In humans, noise has been reported to negatively affect cardiovascular, metabolic and mental health as well as dementia and birth outcomes (Waye and van Kempen, 2021). In specific, noise was associated with cardiovascular diseases (e.g. Dratva et al., 2012; Hahad et al., 2019; Wang et al., 2025), blood pressure and hypertension (e.g. Babisch et al., 2014; Bluhm et al., 2007; Lee et al., 2019; Petri et al., 2021; Pitchika et al., 2017; van Kempen and Babisch, 2012), annoyance and stress levels (e.g. Evans et al., 1995; Marquis-Favre et al., 2023; Miedema and Oudshoorn,

* Corresponding author at: German Aerospace Center (DLR), German Remote Sensing Data Center, Geo-Risks and Civil Security, Oberpfaffenhofen, Germany.
*E-mail address:* jeroen.staab@dlr.de (J. Staab).

https://doi.org/10.1016/j.trd.2025.105063
Received 20 December 2024; Received in revised form 12 September 2025; Accepted 13 October 2025
Available online 21 October 2025

2001; Yadav et al., 2025), sleep quality (e.g. Muzet, 2007; Öhström and Rylander, 1990), cognitive performance (e.g. Erickson and Newman, 2017; Lavandier et al., 2022; Raess et al., 2022; Rossi et al., 2018; H. Xie et al., 2011) and only recently with increased adipose tissue depots and hepatic fat content (Niedermayer et al., 2025). The increasingly urbanized lifestyle of modern societies, technological advancements and economic welfare, however, is seemingly inseparably linked to the constant resonant hum of interconnected systems. Observed in further detail, noise emissions originate from distinct sources (Bolognese et al., 2024; Licitra et al., 2022). These include strong but local effects of airports, disperse distribution of industrial emissions, railways and low frequency vibrations emitted by wind turbines. However, the most prevalent source of noise in Europe is considered to be emitted from running engines and rolling tires – road traffic (European Environment Agency, 2020a).

While the European Union was initially established with an economic focus, it has since taken on an active role in protecting environmental and public health (European Commission, 2021). Actually, even far before the European Green Deal was drafted, the European Commission initiated the strategic mapping of noise and the respective production of noise mitigation plans. The European Noise Directive (hereafter referred to as END, 2002/49/EC), accounts for different sensitivities of noise from different sources during different times of the day. The day–evening–night noise level indicator $L_{den}$ delineates the yearly averaged sound pressure, including weighting penalties for evenings and nights. Its spatial representation is delineated in strategic noise maps, which are produced by engineers using standardized noise simulation methods. For the third mapping round conducted in Germany – 2017, that is the preliminary calculation method for environmental noise on roads (abbreviated in German as VBUS, published by Bundesanstalt für Straßenwesen, 2006). These state-of-the-art noise prediction models incorporate source emission approximation and certified propagation models to predict noise levels in the plane (Khan et al., 2021). While the emissions module approximates the sound pressure levels based on in-situ measurements of different vehicle types at different drive-by speeds on different road surface materials, the propagation modules deploy a geometrical propagation theory. Here, the complex mechanics in acoustics mostly consisting of staggered façade refractions in urban environments and ground surface absorption on different land surface materials are simplified as rays (Garg and Maji, 2014; Steele, 2001).

These standardized noise simulation methods however, bind respective professional and computational resources. With respect to cost-efficiency, the END therefore has some critical limitations. First, due to the fragmented organization of member states and their internal structures, regional noise emission assessments are often delegated to different engineering bureaus conducting the noise mapping. Second, the END requires different level of details for urban agglomerations and peripheral areas. Within agglomerations, defined in Germany as having a population exceeding 100,000 persons and a respectively high population density (BImSchG §47b.3[1]), all roads with $L_{den}$ greater than 55 dB(A) are included. For smaller towns or rural regions though, noise mapping is only mandatory along major roads with more than three million vehicle passages a year. In fact however, polycentric structures, smaller urban patches and suburban areas that have grown beyond the administrative borders (Taubenböck et al., 2019, 2017) are left out. Assessing END compliant noise maps in the context of environmental justice studies, Riedel et al. (2014) concluded, that noise effects on health might be underestimated consequently. On one hand, the associated costs of producing such legally binding strategic noise maps justifies spatial constraints. On the other hand, due to these different requirements, there is no consistent noise exposure map available on a national, let alone international, scale. As a result, nationwide and comparative epidemiological studies lack this information. The number of critically noise exposed people in Germany, for example, is unclear. Referring to the latest available END maps of 2017 for Germany, 8.1 million inhabitants were exposed to road traffic noise values above 55 dB(A) $L_{den}$ (Staab et al., 2025). But, when for example assigning this data to the residential addresses of more than 200,000 participants of the German National Cohort NAKO (Peters et al., 2022), 31 % of the participants lived in regions outside the mandatory END mapping. Consequently, an underestimation of the actual number of exposed participants is assumed by environmental epidemiologists (Wolf et al., 2025).

In a similar context, a complementary approach for mapping noise was adopted from air quality assessments by D. Xie et al. (2011). Land Use Regression (LUR) models utilize geospatial representations of emitting sources and propagation affecting factors such as distance to roads, surface materials and others, in order to gauge noise exposure statistically. The statistical models utilized are most often least square regressions (Aguilera et al., 2015; Chang et al., 2019; Gharehchahi et al., 2024; Harouvi et al., 2018; Kim et al., 2021; Kumar and Garg, 2025; Sieber et al., 2017; D. Xie et al., 2011; Xu et al., 2022) and generalized additive models (Goudreau et al., 2014; Liu et al., 2020; Ragettli et al., 2016), whereas recently, a comparison to random forests was conducted by Liu et al. (2020). The just cited references have all in common, that in-situ microphone measurements were used to sample the reference data. With respect to logistic costs, this does not scale well towards a nationwide scope, intended with this study. Building on high correlations between in situ noise measurements and such END compliant noise maps (Aguilera et al., 2015), several studies (Sharma et al., 2024; Eicher et al., 2022; Staab et al., 2022, 2023) have independently investigated the potential of using END compliant reference data for large-scale extrapolations. Thereby, the source specificity of strategic noise maps (i.e. road traffic noise) and the annually averaged sound pressure indicator $L_{den}$, correspond to the static nature of non-multitemporal geodata.

Aiming to identify disparities in transportation noise exposure (Tang and Li, 2024), this study addresses both, the spatial limitations and federal heterogeneity inherent to current noise END-conform mapping products. The goal of this study is to combine the potential of multimodal geographic data in combination with machine learning techniques to model road traffic noise on a large scale. Thereby, the distinct advantages of geoinformation processing tools and recent high-performance computing power are leveraged to produce a high-resolution noise map for the complete landmass territory of an exemplary country at 10 x 10 Meter resolution. Germany was chosen for logistical reasons and a wide band of key factors – a differentiated road network, heterogenous landscapes transitioning

[1] https://www.gesetze-im-internet.de/bimschg/__47b.html.

from flat northern areas to the mountainous regions in the south and various degrees of urbanization. Aiming for a well generalizing map, repeated spatial cross validations (as in Staab et al., 2022) are used to evaluate the transfer learning approach (Pan and Yang, 2010).

The remainder of this study will delineate the experimental setup, analytical framework and collected data, first. Then, the result section does highlight both, the benchmarked model performances with respect to accurate predictions and computational footprint, as well as the first national road traffic noise map having set consistent parameters for all 357,689 $km^2$ and 82,792,351 inhabitants[2] respectively. Eventually, the implications of the findings are discussed before conclusions are drawn that contribute to the understanding of road traffic noise exposure in Germany.

## 2. Research design

Both, the analytical approach and data processing workflow are outlined in Fig. 1. First, official noise maps are selected and sampled (highlighted green in Fig. 1). Next, experiments are set up to tune a respective machine learning model (highlighted orange), where different hyperparameter sets are trained and tested on their spatial transferability (Pan and Yang, 2010) in order to produce an accurate and robust model. Focusing on the average road traffic noise levels $L_{den}$ reported in 5 dB(A) contours only, a LUR approach (Aguilera et al., 2015; D. Xie et al., 2011) was adapted to an ordinal scaled classification problem, where two different ensemble learning techniques will be compared to harmonize and extrapolate the selected strategic noise maps. The machine learning task is backed by a set of 82 complementing predictor variables engineered to scope – analog the conventional noise prediction models – factors associated to sound emission, as well as variables describing the environment propagating sound wave interact with (highlighted blue). The experimental setup itself is conducted on a high-performance data analyses cluster. Thus beyond the conventional measures of accuracy and model robustness, the benchmarks retrieved from the workload manager quantify the utilized resources across the hyperparameter, such that the accuracy of each model can be traded off against its economic and ecologic footprint (Schwartz et al., 2020). The best model is eventually deployed on the nationwide feature collection, producing road noise information at a 10 x 10 Meter resolution. A nationwide exposure analysis (highlighted yellow) demonstrates the applicability of this study.

## 3. Strategic noise maps

With respect to individual strategic noise maps being produced using certified approaches and suitable for legal matters, they are credited a high semantic accuracy. The noise data delineates areas exposed to $L_{den}$ values between 55 and 75 dB(A) in 5 dB(A) intervals.

Using this entry point, the most recent data for urban agglomerations published as part of the 2017 reports was accessed. These are 71 different shapefiles reported by individually responsible cities and federal states. However, the data retrieved via the European Environmental Agencies EIONET platform comes at varying qualities (Khomenko et al., 2022). While originally, noise is simulated at grid cells ($\leq$10 Meter resolution), the reported shapefiles often were produced with simplified geometries – at the costs of local details (Staab et al., 2025). To ensure high data quality and avoid potential bias introduced during postprocessing, we selected only those 21 cities where original raster layout properties was retained (see Table S1).

Pooled together, they cover a total area of 3,840 $km^2$ as reference data – whereby 32.5 % of the area (i.e. 1,248 $km^2$) are exposed to $L_{den}$ values above 55 dB(A). As the variance in noise levels is proportional to traffic flow and the surrounding environment, neighboring pixels are prone to spatial autocorrelation. The number of reference samples was therefore limited to one million pixels (i.e., 100 $km^2$). These samples (referred to as virtual microphones in Staab et al., 2022), are stratified across land use classes derived from the European Urban Atlas (European Environment Agency, 2020b) and proportionally balanced between the 21 cities. This decision was guided by Staab et al. (2022), who found that explanatory contributions converge at very large sample sizes and that the informative value of a reference point depends on the spatial context. Thereby, the balanced stratification prepares the reference data for structured cross validations (Roberts et al., 2017), later. Compared to the total area (c. f. Table 1), the samples carefully overrepresent the otherwise only rare patches above 65 dB(A), such that these critical areas are fair to be learned by the machine learning algorithm (He and Garcia, 2009).

## 4. Experimental setup

Compared to conventional LURs using least squares, random forests can achieve higher accuracies (Helbich et al., 2025; Liu et al., 2020). This ensemble learning algorithm introduced by Breiman (2001) can be applied on regression problems, i.e. modeling a continuous target variable, and classification problems such as modeling discrete target classes with 5 dB(A) $L_{den}$ intervals in this prevalent case. The predictions of numerous non-parametric decision trees are aggregated. By selecting random subsets of the training data and variables when building each tree – a process called bootstrap aggregation or "bagging" – random forests can adeptly manage multicollinearity and complex interactions between input features (Belgiu and Drăguţ, 2016). Aiming for an ideal model configuration, hyperparameters can be used to finetune the learning process. Here, the high fidelity of noise in diverse landscapes requires a model that is sensitive to multimodal feature interaction. Opposed thereto, overfitting must be avoided to ensure a robust spatial

[2] https://daten.gdz.bkg.bund.de/produkte/dlm/dlm250/2017/.

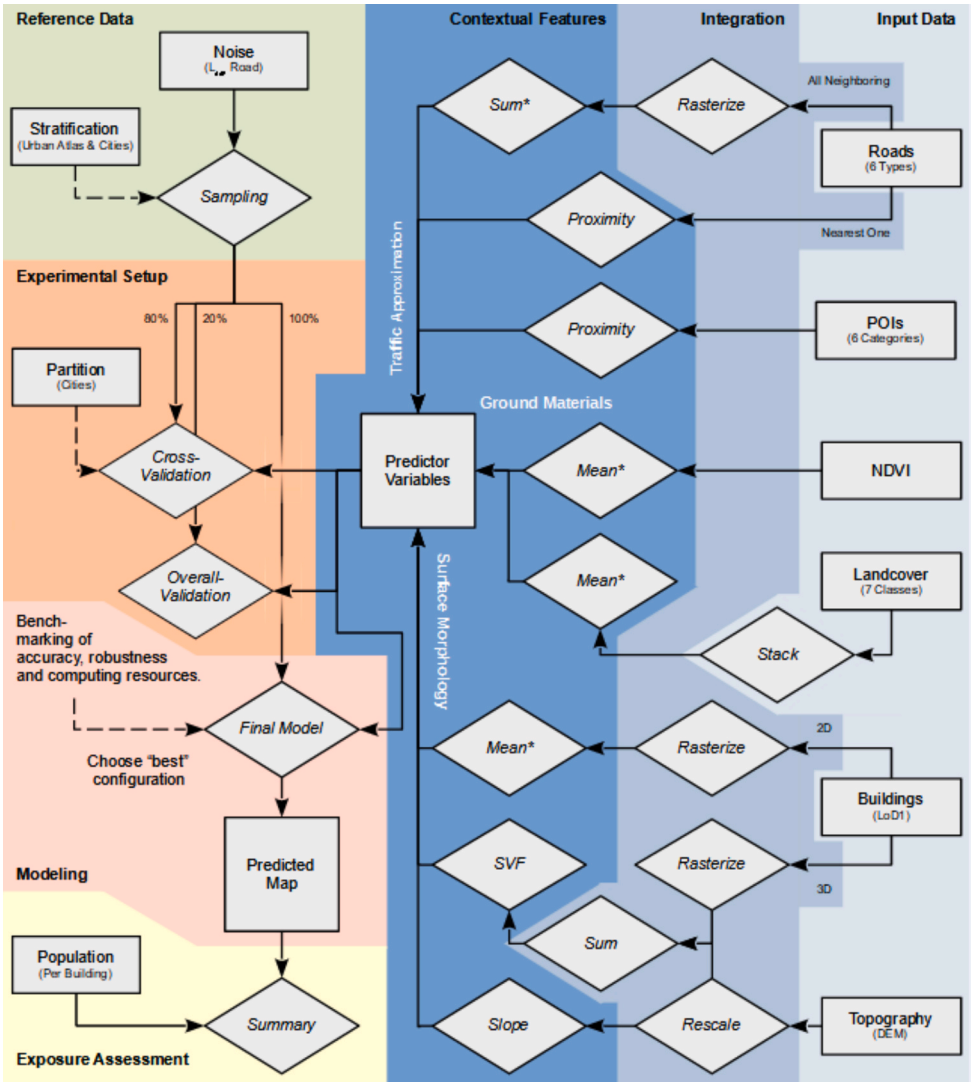


**Fig. 1.** Flowchart categorizing data (shown as rectangles) and techniques (represented by rhombuses) into primary procedural stages (highlighted with colored backgrounds). Solid black connectors depict the primary data trajectory, while dashed connectors indicate supplementary information flow relevant to control the specific techniques. Annotated rhombuses with asterisk (*) utilize moving window operators with 30, 100, 300 and 1,000 m radii. Abbreviations: POI = Points Of Interest, NDVI = Normalized Difference Vegetation Index, LoD1 = Level of Detail 1 building model, DEM = Digital Elevation Model, SVF = Sky View Factor, CV = Cross Validation.

**Table 1**
Statistical summary of sampled, END compliant, road $L_{den}$ data.

| | *Area* | *Fractional cover per road $L_{den}$ interval in dB(A)* | | | | | |
|---|---|---|---|---|---|---|---|
| | | *< 55* | *55 < 60* | *60 < 65* | *65 < 70* | *70 < 75* | *≥ 75* |
| *21 Cities* | *3,840 km²* | *67.5 %* | *13.0 %* | *8.7 %* | *5.6 %* | *3.1 %* | *2.0 %* |
| *Samples* | *100 km²* | *64.4 %* | *12.1 %* | *8.7 %* | *5.7 %* | *3.5 %* | *4.6 %* |

transferability. Therefore, a systematic tuning of hyperparameters (Yu and Zhu, 2020) is benchmarked.

### *4.1. Random forest hyperparameters*

With respect to its optimized runtime and exposed hyperparameters in the *R* (R Core Team, 2023) package *caret* (Kuhn, 2008), the *ranger* implementation by Wright and Ziegler (2017) was utilized. The training of the ensemble learning model is controlled by several hyperparameters which exert influence on the model accuracy and robustness. Keeping the number of trees constant at 500, special

attention was accorded to the selection of the three hyperparameters *splitrule*, *minnodesize* and *mtry* to trade of local accuracy versus model generalization. A detailed grid search process (Yu and Zhu, 2020) was carried out, allowing us to evaluate and compare a total of 88 different hyperparameter sets against each other.

- The *splitrule* governs how splits in the decision trees are determined at each node. For conventional random forests, the Gini index measures the impurity of a node in the tree and strives to maximize the homogeneity within each node created by a split. Conversely, the ExtraTrees method chooses thresholds for each feature randomly intended to increase the model robustness.
- The *minnodesize* parameter defines the minimal number of observations required in a node to consider further splitting. This harmonizes the model complexity against the predictive performance. While a smaller *minnodesize* value allows the trees to grow deeper, this potentially leads to overfitting to the training data. Conversely, a larger value promotes model generalization by preventing the creation of nodes that only refine predictions for a negligible portion of the data. However, it could also underfit to subtle acoustical phenomena. Aiming for an accurate but robust model, this hyperparameter was tuned along the exponential gradient stretching from *minnodesize* being either 1, 10, 100 to 1,000.
- Within the context of the multimodal features engineered, the tuning parameter *mtry* is of particular importance. This parameter defines the number of features randomly sampled at each node in the tree from which the best feature for a split can be selected. For most cases, the floored square root of the number of predictors is suggested (Breiman, 2001). However, a larger value increases the chance, that relevant variables are selected during the splitting procedures. With regards to interaction effects, *mtry* controls the model's ability to capture intervariable relationships. The systematic tune grid testing *mtry* being either 3, 6, 8, 9, 10, 12, 15, 20, 30, 50 or 80 is denser around the recommended value but experiments extreme settings as well.

### 4.2. Benchmarking

Optimal hyperparameters were selected based on the highest weighted Kappa (Cohen, 1968). This modification expands Coheńs Kappa to measures the degree of disagreement as well – relevant for ordered ordinal data. Implemented by Gamer et al. (2019), the disagreements are weighted according to their squared distance from perfect agreement. With respect to noise exposure, this means that smaller confusions to neighboring noise bands ($\pm$5 dB(A) $L_{den}$) have smaller weights compared to larger estimation errors. The accuracy is benchmarked for both, a cross validation using 80 % of the sampled virtual microphones, as well an overall validation using 20 % held-out ones. Along thereto, the computational resources consumed per experimental configuration is logged. Eventually, these complementing metrices allow to search for the most suitable model configuration.

#### 4.2.1. Cross validation

In the analytical framework, the present study emphasizes the robustness and transferability of the prediction through specialized cross validation. This technique aims to assess the model's generalizability by partitioning the data into complementary but independent subsets, training the model on one subset, and validating it on the other. For inherently structured spatial data this concept can be challenged due to spatial autocorrelation (Roberts et al., 2017). Accordingly, the CV was partitioned based on spatial divisions analog to Staab et al. (2022). That is, one city is left out during each CV iteration – referred to as Leave-Spatial-Out-Cross-Validation ($LSOCV_{Admin}$). This ensures that the model is consistently evaluated against independent spatial entities and measure the spatial transferability of the model, which is pivotal in gauging its predictive performance across various administrative zones and large-scale application.

Although the maps adhere to the END framework methodological variation is expected due to differing software tools and the interpretive flexibility allowed by the Good-Practice-Guide (WG-AEN, 2007). Therefore, the outputs are not always congruent when comparing the geospatial data along each other (cf. Staab et al., 2025). While it is not possible to qualify the individual noise maps – in particular if they are not sharing an administrative boundary – the data driven approach is able to identify respective outliers. That is, the accuracy of a $LSOCV_{Admin}$ iteration deviates, if a particular region used for validation has applied different standards compared to the other regions used for training. A descriptive scatterplot is used to visualize the individual accuracies achieved during the CV iterations, along the respective mean, standard deviation and density curve highlighting the distribution.

#### 4.2.2. Model robustness

A priori, the reference samples were split, keeping out 20 % as an overall validation data set. For each model tuned, the weighted Kappa was calculated to evaluate the modelś generalization to unseen data. The discrepancy between overall- and cross validation was used to indicate overfitting (Chang et al., 2019; Roberts et al., 2017). The absolute difference between both weighted Kappa values is hereafter referred to as measure of robustness.

#### 4.2.3. Computational resources

With respect to the vast amount of training samples, features, hyperparameter sets, 21 cross validation iterations and the computation of one last overall model, respective computation resources were required. High Performance Computing (HPC) has emerged as a pivotal tool to analyze vast datasets of geospatial data, too (Lee et al., 2011). It was therefore relied on the *terrabyte* cooperation between the German Aerospace Center (DLR) and the Leibniz Supercomputing Center (LRZ), Garching, Germany. For managing and orchestrating computations, the workload manager SLURM is used to efficiently harness the power of the highly parallelizable high-performance data analytics (HPDA) cluster. Each hyperparameter configuration was evaluated in a dedicated job, allocating 20 CPU cores and 100 GB of RAM for 48 h each. Once a job was finished, a report was generated summarizing the utilized

resources. This allowed us to assess the actual consumed computational resources per hyperparameter tuning experiment. Both metrics were annotated to the experiments' accuracies, for a conclusive cost-benefit trade-off.

#### 4.2.4. Model selection

To identify the most suitable model for a nationwide deployment, two options were considered and compared: (a) the best performing model based on the highest weighted Kappa during the cross validation, (b) the most robust model configuration based on the smallest absolute difference between both cross-validated and overall validated weighted Kappa value analog to Staab et al. (2022), as well as (c) the most computational effective. Without directly trading off utilized CPU hours and gigabyte of memory consumption, each benchmark was independently ranked, and the resulting ranks were then combined to calculate an overall efficiency score. The experiments with the lowest cumulative rank are considered the most efficient. Eventually, the selected models are deployed to exemplary regions of interest, in order to conduct a qualitative assessment. Therewith, a broader understanding of how the models perform is gained.

### 4.3. Predictor variables

#### 4.3.1. Spatial harmonization concept

To provide a representative depiction of noise relevant features to the machine learning algorithm, a catalog of traffic infrastructures, land surface properties, topography and built-up morphology features was compiled. The data mining and feature engineering pipeline thereby consist of three steps (c. f. blue background shades in Fig. 1). First, the input data retrieved from earth observation, volunteered geographic information and public authorities was sourced, and then, second, integrated into a common, 10 x 10 Meter resolution raster stack. Third and most important with respect to the spatial propagation of noise, contextual features were engineered. Either, by applying moving window operators aggregating mathematical functions within the chosen radii of 30, 100, 300 and 1,000 m, or proximity features searching for the nearest occasion around. After engineering the features described below, a total of 82 variables was available for the experiments (see S2 for tabular overview).

#### 4.3.2. Traffic approximation

Most important for such a source specific noise map are both road infrastructure network quality and quantity. A large-scale database of roads for Germany was derived from OpenStreetMap[3] (OSM). In addition to the spatial layout of streets proxy information of traffic volume capacities and speed limits are encoded in the functional road types *Motorway*, *Trunk*, *Primary*, *Secondary*, *Tertiary* and *Residential* (Staab et al., 2022). Encoded as dummy variables (Suits, 1957), the information for each road type was introduced in two complementing parameterizations commonly utilized in such applications – the cumulated road length of all neighboring roads (Aguilera et al., 2015; Chang et al., 2019; Goudreau et al., 2014; Liu et al., 2020; Ragettli et al., 2016; Sieber et al., 2017; D. Xie et al., 2011; Xu et al., 2022) and proximity (Harouvi et al., 2018; Staab et al., 2023, 2022; Xu et al., 2022). Where, **proximity** describes the inverse distance to the nearest road segment of each OSM class, measured in meters. Along these gradients, sound levels are known to decline on a logarithmic basis (Ostashev and Wilson, 2015). Given the use of non-parametric models in this study, these features were not log transformed. Complementary, the **cumulative road length** considers multiple emitting roads in close vicinity and highlights intersections – where noise levels are known to rise in particular (Pascale et al., 2024; Yadav et al., 2025, 2022). The subjacent length of all roads multiplied by their respective number of lanes (WG-AEN, 2007) inside the four moving windows predefined by the spatial harmonization concept.

Also, dedicated **points of interest (POIs)** can attract traffic flows and affect the local soundscape (De Coensel et al., 2005; Karges et al., 2025, 2022; Pascale et al., 2024; Thorsson and Ögren, 2005). Following Harouvi et al. (2018) and Xu et al. (2022), the proximity to local amenities queried from OSM was computed as a proxy for local variance in traffic (see Table S2). Then, referring to the spatial harmonization concept, the proximity to the nearest POI was computed for each category separately.

#### 4.3.3. Ground materials

Propagating sound waves interact with the ground surface (Attenborough, 2007). While plain and solid surfaces such as water bodies and some artificial materials like tarmac have reflecting acoustical properties, soft or porous material have absorbing effects (Aylor, 1972; Piercy et al., 1977). Grass, bushes and other vegetative parts of plants are known to effectively prevent noise from traveling large distances (Aylor, 1972; Margaritis and Kang, 2017; Reethof, 1973). From an earth observation perspective, this photosynthetically active biomass can be approximated with the **Normalized Difference Vegetation Index (NDVI)** to some degree (Huang et al., 2021). Following up the study designs by Goudreau et al. (2014), Sieber et al. and (2017), Ragettli et al. (2016) and Xu et al. (2022), this spaceborne measurement was added to the feature catalog as follows. First, based on all Sentinel-2 images captured between 2015–06-27 and 2017–09-29 with a respective cloud cover below 60 %, a median mosaic was composed using Google Earth Engine (Gorelick et al., 2017). The contextual features were then engineered using radial filters in order to inform the pixel-based approach about the mean NDVI within the surrounding environment.

Scoping a wider range of ground surface materials, **land-cover fractions** were derived as well. In a preceding work, Weigand et al. (2020) distinguished seven land-cover classes: solid surfaces such as *Artificial Land*, *Open Soil* and *Water Areas;* and, as sound

[3] https://openstreetmap.org.

attenuation is proportional to biomass (Margaritis et al., 2018; Reethof, 1973) and highly relevant for noise modelling as well, detailed information on *Low Perennial*, *High Perennial*, *Low Seasonal* and *High Seasonal Vegetation*. At first, this land-cover classification was translated to a feature stack by splitting each class into a separate binary mask. Contextual land cover fractions were then computed for each layer using the four moving windows. Encoded as percentages, for each pixel, the stack of seven features thus condenses the proportion of ground materials within the given radius.

#### 4.3.4. Surface morphology

Above the plane, topography and built-up structures affect the corresponding sound propagation (Heutschi, 1995; Wang and Kang, 2011). To include urban morphologies, both building footprints and building height are added to the model from the nationwide Level-of-detail 1 (LoD1) building dataset as provided by the *Federal Agency for Cartography and Geodesy*.[4] **Open Space Ratio (OSR)** puts the non-built-up areas in proportion to the larger spatial context and is derived from the building footprints only. A low value results from densely built-up areas, while a larger ratio indicates a long and unrestrained propagation of the sound waves. Although this indicator neglects the three-dimensional physics of sound, Silva et al., (2018) stress its relevance for noise.

With respect to the three-dimensional physics of sound, topographical data, Copernicus GLO-30[5] acquired through the TanDEM-X radar mission between 2011 and 2015, was rescaled to the common 10 x 10 Meter resolution using bilinear interpolation and subsequently combined with the built-up model to enhance its vertical resolution. This new dataset actually depicts the topographic volume not available for the expansion of sound pressure. For each pixel, it was aggregated into the **Sky-View-Factor (SVF)** using the HORIZON package (Van doninck, 2018), delineating the ratio of visible sky not blocked by obstacles (Dozier and Frew, 1990).

Last but not least, the topography can affect the emitted road traffic noise levels as well (Xu et al., 2023), which is particularly the case for vehicles with combustion engines ascending (Beckenbauer, 2013). Paraphrasing the official noise simulation input parameters (Müller and Bartolomaeus, 2015), **slope** was derived based on the rescaled GLO-30 dataset as well.

### 4.4. National application

After a thorough investigation of the benchmarked hyperparameter configurations, the most suitable model is deployed nationwide.

Eventually, the generated data is used to answer the previously posed question, of how many inhabitants in Germany are exposed to noise. Therefore, the latest 100 x 100 m resolution census grid[6] is disaggregated to household levels (analog to Staab et al., 2025). Zonal statistics then aggregate the critically exposed population per noise band. For a better comparability to the exposure counts based on previous status-quo-data, the values are represented as relative proportions of the total population.

## 5. Results

To establish a consistent estimate of road traffic noise exposure in Germany, this study was framed as a machine learning challenge, which must be evaluated first. The most suitable models are investigated in detail, such that beyond the optimal model choice, the strengths and weaknesses of statistical approach for mapping noise become clear. Eventually, the national inference is used exemplary, in order to answer the initial question, of how many inhabitants are exposed to critical noise levels.

### 5.1. Hyperparameter tuning

The weighted Kappa coefficients for the different models and hyperparameters are compared in Fig. 2. Circles annotated with vertical error bars indicate the results of the spatial cross validation. The overall validation scores are represented with x-markers. In particular, at smaller *mtry* settings (X-Axis), the default *splitrule* Gini (red) produces higher accuracies than using randomized splits using ExtraTrees (turquoise). Beyond the recommended *mtry* settings of 9, the benchmarked coefficients of agreement converge. With respect to the overall validation, the achieved weighted Kappa values are systematically higher. At the same time, the weighted Kappa values achieved during the overall validation are lower at larger *minnodesizes*. As the discrepancy between cross- and overall validation with held-out samples shrinks, more robust models can be found when reading the figure from left to right.

While in summary, the parallel evaluation of the experimental setup consumed 1.8 terabyte of RAM on 392.1 days of CPU wall-clock time, the respective utilized resources per experiment did highly depend on the selected hyperparameters – two in particular. As shown in the second row of Fig. 2, the CPU hours are linear proportional to *mtry*, where the width of trees increases the computational efforts. At the same time, experiments with smaller *minnodesize* require more gigabytes of RAM, as deeper trees are built. The *splitrule*, has neglectable effects on the computational costs.

Searching for the most suitable model to be deployed nationwide, four hyperparameter configurations stand out (Table 2). On the one hand, a), Experiment 41 with *mtry* set to 12, *splitrule* being Gini and a *minnodesize* of 1 achieved the highest weighted Kappa during overall validation with 20 % left out samples. On the other hand, b), Experiment 88 with *mtry* set to 80, *splitrule* being ExtraTrees and a very large *minnodesize* of 1,000 had the highest measured robustness, with the absolute difference between overall- and cross-validated

[4] https://gdz.bkg.bund.de/index.php/default/digitale-geodaten/sonstige-geodaten/3d-gebaudemodelle-lod1-deutschland-lod1-de.html.
[5] https://doi.org/10.5270/ESA-c5d3d65.
[6] https://www.zensus2011.de.

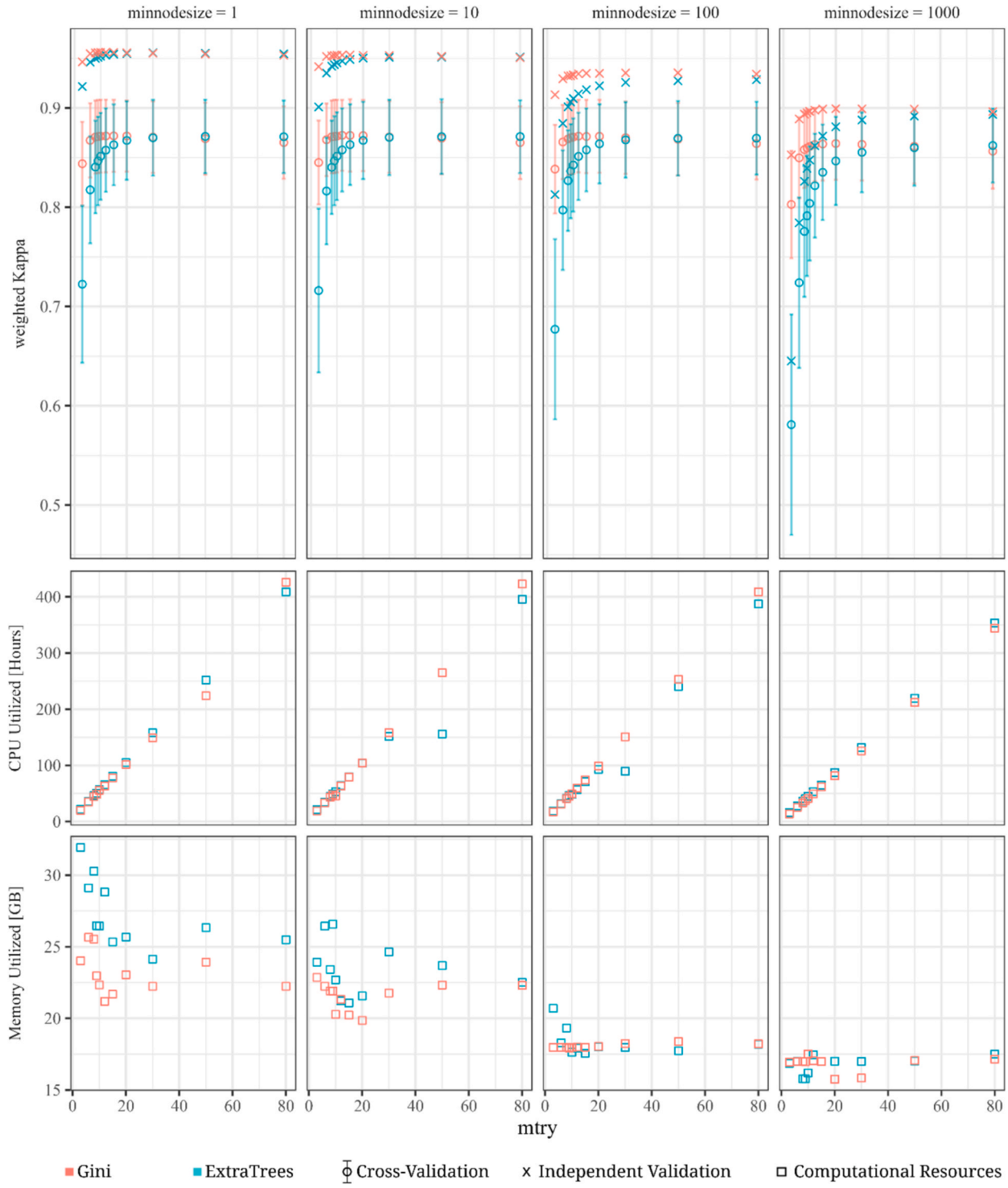


**Fig. 2.** Evaluating different aspects of the hyperparameter tuning (facets by rows) across the random forests parameters splitrule (colors), minnodesize (facets by columns) and mtry (X-Axis). The first row depicts the weighted kappa values, where the cross-validated means are represented as circles annotated with error bars, while x-markers represent the overall validation. The two rows below delineate the computational resources consumed by the respective SLUM jobs evaluating each configuration individually.

**Table 2**
Detailed benchmarks for selected experimental hyperparameter sets. Experiment 15 scored first with respect to average computation resources utilized. Experiment 41 achieved the highest weighted Kappa during overall validation with 20 % left out samples. Whereas Experiment 88 is considered being the most robust, as it had the least difference between weighted Kappa during CV and overall validation.

| *Exp. ID* | *splitrule* | *minnodesize* | *mtry* | *weighted Kappa Cross Validation Mean ± Standard Deviation* | *Overall Validation* | *CPU Hours Utilized [Rank]* | *GB Memory Utilized [Rank]* |
|---|---|---|---|---|---|---|---|
| *Exp. 15* | *Gini* | *1000* | *6* | *0.850 ± 0.041* | *0.889* | *25.32 [1]* | *16.98 [9.5]* |
| *Exp. 41* | *Gini* | *1* | *12* | *0.872 ± 0.037* | *0.956* | *63.29 [57]* | *21.19 [49]* |
| *Exp. 88* | *ExtraTrees* | *1000* | *80* | *0.862 ± 0.037* | *0.893* | *353.36 [46]* | *17.50 [21]* |

weighted Kappa being only 0.031. Experiment ID 15 ranked as computation most efficient. Its small *mtry* parameter set required typically few CPU hours, while the use of the Gini splitrule kept the memory consumption low.

Inspecting the three selected models visually provides further insides, on how the models cope with the very details of actually predicting noise levels. S3 shows three examples ranging from a highly urbanized area with many different roads on a small patch, towards a motorway intersecting a wide and open landscape. Thereby, two trends can be delineated. First, with respect to the very fine details of the contour bands, the broader generalization of larger minimal node sizes becomes apparent. Also, the distinct nuance of a residential road either going through an industrial area and therefore most probably being louder than any other residential road is difficult to capture at large node sizes. Second, the logarithmic nature of sound dispersions inherits, that very loud areas most probably are encapsulated by wider bands of lower noise levels. However, in particular the two configurations with a large *minnodesize* fail painting this hierarchical design typical for strategic noise maps and spare out wide areas affected by noise levels in between 55 and 60 dB(A).

### 5.2. Spatial transferability

A detailed look onto the CV's error bars length (presented in Fig. 2 above) shows them only decreasing to some extent. The large variability at smaller *mtry* parametrizations is plausible, as here, the random forests heavily rely on the random subset of selected variables, although the complex acoustical mechanisms can only be scoped by their wide and multimodal interactions. The errors do however, stay consistent if set $mtry \geq 20$. As the data contains variance beyond the explanatory scope of the features the $LSOCV_{Admin}$ iterations must be scrutinized. Excluding always one individual city during the 21 respective cross validation iterations, allows to assess the spatial transferability to unseen regions. For the three selected experiments the following Fig. 3 depicts the weighted Kappa values achieved for each iteration, where – for the outliers – the city validated against is named. In despite of the respective hyperparameter configuration, all three experiments show a longer left-skewed distribution. Interestingly, Halle (Saale) and Offenbach am Main consistently showed the lowest weighted Kappa. This indicates that in these two cities, the strategic noise maps include patterns, which cannot be learned elsewhere. In contrast, when training with all cities but Darmstadt, the respective accuracy was highest. Transferring a pretrained model to this city in southern Hesse thus works particularly well.

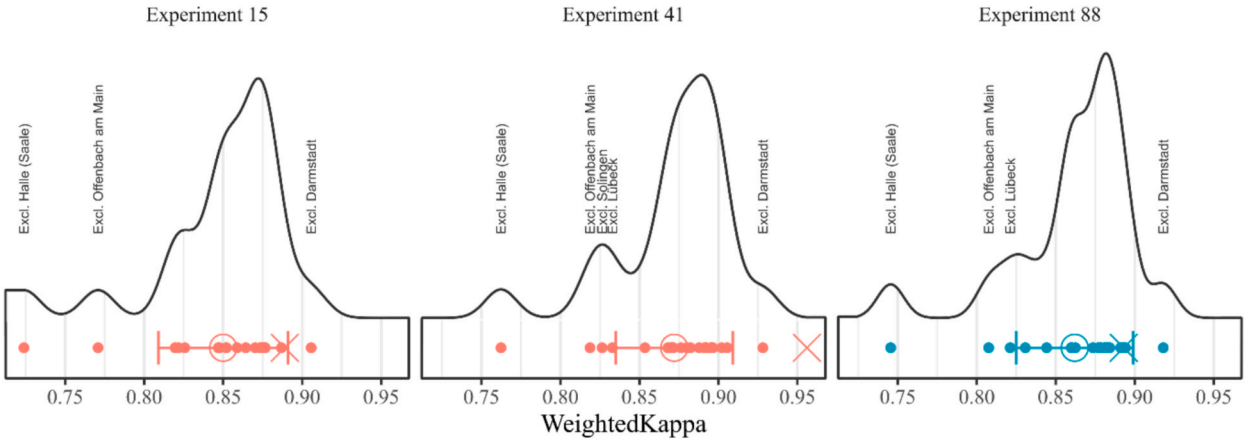


**Fig. 3.** Detailed view of selected experiments for weighted Kappa values (X-Axis) achieved during spatial cross- and overall validation. Analog to Fig. 2, circles represent the cross-validated means along error bars annotating the standard error, while x-markers represent the overall validation and red (Gini) and turquoise (ExtraTrees) are used to distinguish the random forests parameters splitrule visually. Moreover, small dots represent the individual the $LSOCV_{Admin}$ iterations, where the excluded city is labeled above the X-Axis, if outside the standard error. The plots upper contour itself corresponds to the respective kernel density.

### 5.3. National application

Based on the overall evaluation, the best performing model (Experiment 41), was applied to the descriptive raster data prepared for the entire country in order to produce the first national road traffic noise ($L_{den}$) map. It expands beyond the 21 reference cities to the entire country and thus provides noise exposure analyses for the national extent which, based on the END mandated maps, was unattainable before. It depicts noise exposure consistently for the entire population of Germany.

#### 5.3.1. Class specific accuracy

When comparing the final model trained with the combined reference data of all 21 cities against the 20 % held-out samples, an overall accuracy of 90.7 % was computed. The error matrix (Table 3) furthermore specifies the noise band specific errors. Both, User- and Producer Accuracy certify a performance beyond 90 % correct classified pixels for areas of low noise exposure below 55 dB(A) $L_{den}$ and for highly exposed areas above 75 dB(A). There are, however, some misclassifications in the intermediate range. Referring to the in total 11,962 samples in the upper right diagonal half, 5.99 % of the areas officially exposed to road $L_{den}$ values between 55 and 75 dB (A) have the tendency of being predicted as to quiet. In detail, most of these confusions concern the neighboring noise interval classes. *Id est*, the error is usually less than 5 dB(A) $L_{den}$ too quiet in 4.86 % of the cases. Vice versa, 2.90 % are less than 5 dB(A) too loud. In summary, 7.8 % of predictions exhibited deviations within $\pm$ 5 dB(A). Only in 1.57 % of the held-out samples are predicted to be more than $\pm$ 5 dB(A) wrong.

#### 5.3.2. Geographical assessment

In Fig. 4, the predicted noise levels across Germany (a) are presented. Three zooms illustrate the model's capability along the gradient from urban to rural environments. Panel (b) provides an overview of the larger geographic setting surrounding Berlin. The dense and noise street network expands outwards from the city center along the major roads and highways. In between, a fine street network exhibits a dendritic pattern, with main roads branching into finer streets interconnecting suburban clusters. Panel (c) focuses on the north eastern administrative boundary of Chemnitz to exemplify the model's performance to extrapolate road traffic noise outside the bounds of the reference data. Smaller roads not scoped by the END article 3 section *n* conventionally are not considered in official noise maps. This demonstrates, that the predictive framework can contribute to suburban settings, where such data is often sparse or incomplete. The same argument is true for smaller towns, illustrated in panel (d) for Landsberg am Lech.

#### 5.3.3. Exposure assessment

With respect to the 82,792,351 individual's exposure in Germany, the noise values were assigned to the living addresses. Table 4, depicts the aggregated share of population per predicted noise interval class. For comparison, the data is shown for the officially reported noise maps (data published along Staab et al., 2025) as well. The most prominent difference refers to the majority of people, whom where previously living outside of urban agglomerations concerned by the obligation defined in END Article 3 Sec. n and unaffected by noise emitted along major roads with more than 3 million vehicle passages per year (END Article 3 Sec k). But also, the combined share of 78.5 % + 11.2 % = 89.7 % is smaller, compared to our prediction. Here, only 84.1 % of the population was assigned into the lowest noise exposure class. This increase spreads uneven beyond the different noise bands, as in particular the share of population exposed to 65 < 70 dB(A) rises by factor 2.5 and factor 6 for the population share exposed to 70 < 75 dB(A) respectively.

Summarizing the shares above 55 dB(A), we have predicted 15.9 % of the total population are exposed to critical road traffic noise levels above 55 dB(A) $L_{den}$. In absolute terms, this are 13.1 million people. Along the previously known 8.5 million inhabitants exposed to road $L_{den}$ values beyond 55 dB(A), 4.6 million inhabitants are thus considered to be exposed to critical, yearly averaged road traffic noise during day, evening and night in Germany as well.

## 6. Discussion

Noise is considered harmful for different aspects of health (European Environment Agency, 2020a). However, the official, cost-optimized datasets are unsuitable for large-scale epidemiological assessments. Closing this gap, a nationwide noise prediction

**Table 3**
Confusion matrix assessing the accuracy using 20 % held-out samples. Top row delineates referenced noise bands ranging from < 55 dB(A) up to > 75 dB(A) in five dB(A) steps. Respectively, first column delineates predicted noise level intervals. In cells, the absolute number of referred pixels is delineated. Correct predictions are aligned along the diagonal (highlighted bold), whereas above, the predicted noise levels are too quiet. Cells below the diagonal are predicted to be louder and thus more harmful than the official reference.

| *Confusion Matrix* | | *Reference [Lden dB(A)]* | | | | | | *User Accuracy* |
|---|---|---|---|---|---|---|---|---|
| | | *<55* | *55 < 60* | *60 < 65* | *65 < 70* | *70 < 75* | *>=75* | |
| *Prediction [Lden dB(A)]* | *<55* | ***126.841*** | *4.589* | *1.295* | *550* | *127* | *16* | *0.951* |
| | *55 < 60* | *1.527* | ***20.017*** | *1.779* | *123* | *13* | *1* | *0.853* |
| | *60 < 65* | *252* | *1.448* | ***12.900*** | *1.474* | *81* | *3* | *0.798* |
| | *65 < 70* | *155* | *142* | *1.259* | ***8.124*** | *1.254* | *42* | *0.740* |
| | *70 < 75* | *69* | *27* | *73* | *885* | ***4.792*** | *631* | *0.740* |
| | *>=75* | *9* | *6* | *34* | *119* | *686* | ***8.656*** | *0.910* |
| *Producer Accuracy* | | *0.984* | *0.763* | *0.744* | *0.721* | *0.689* | *0.926* | |

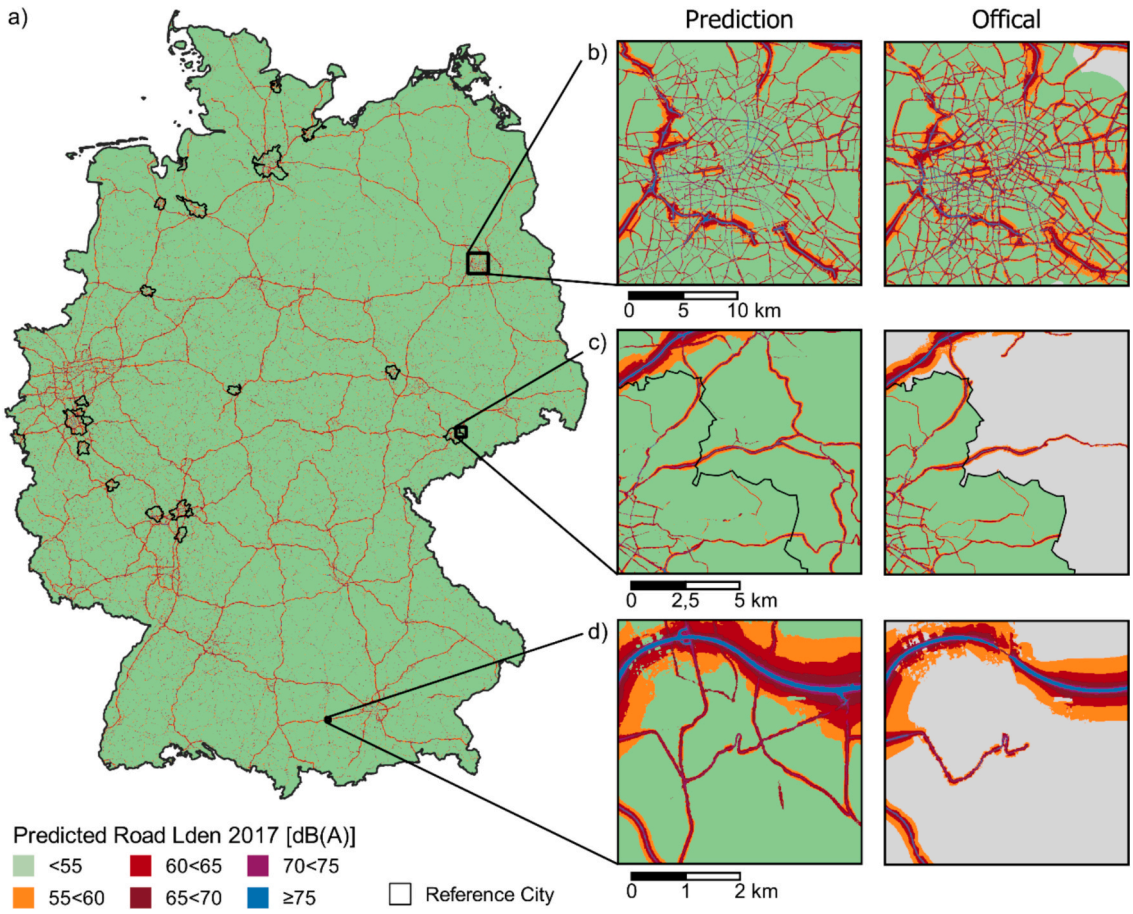


**Fig. 4.** Predicted noise levels for Germany. Zooms along the urban–rural gradient show (b) the city of Berlin in its extended spatial context, (c) continuous extrapolation of road traffic noise outside reference data – exemplified for the city of Chemnitz, and (d) noise being mapped for smaller towns as well – here the city of Landsberg am Lech with 28,865 inhabitants in 2017. For reference, the official noise predictions are shown to the right.

**Table 4**
Summary of exposed population to road $L_{den}$ [dB(A)] in Germany. Total population is 82,792,351.

| | *No Data* | *<55* | *55 < 60* | *60 < 65* | *65 < 70* | *70 < 75* | *>=75* |
|---|---|---|---|---|---|---|---|
| *Official* | *78.5 %* | *11.2 %* | *5.9 %* | *2.8 %* | *1.5 %* | *0.1 %* | *0 %* |
| *Prediction* | *0 %* | *84.1 %* | *6.6 %* | *4.9 %* | *3.8 %* | *0.6 %* | *0 %* |

pipeline utilized a fine-tuned random forest in order to aggregate high dimensional descriptors of the urban- and natural environment. In congruence to the legal obligations, a road traffic specific assessment was produced by building upon the work of Staab et al., 2022, 2023), Eicher et al. (2022) and Sharma et al. (2024). As strategic noise maps are usually reported in ordinal scaled intervals (Khomenko et al., 2022), this research adapted the commonly used land use regression algorithms to perform an ordinal scaled classification. Thereby, the experimental setup using a spatial cross validation was able to compare cities against each other, although physically, not sharing an administrative boundary. Herewith, a unique perspective on the intersection of machine learning and administrative responsibilities is provided. By maintaining a consistent mapping approach across the entire study area and applying the same parameterizations, our predictions remain sovereign in the face of administrative obligations and responsibilities. This approach not only ensures the reliability of our nationwide results but also facilitates direct comparisons throughout the study area. Therewith, the presented noise estimated can be used to improve the noise exposure assessment and enable subsequent epidemiological analyses with Germany's largest population-based cohort study (Wolf et al., 2025), for example.

However, the statistically estimated results presented above need to be carefully interpreted. With respect to health effects, the utilized noise indicator $L_{den}$ blurs the periodical amplitude of highly impulsive sound sources where penalties might be required (Kukulski and Wszołek, 2022; Rajala and Hongisto, 2020; Virjonen et al., 2019). But also, the WHO strongly recommend to reduce road traffic noise $L_{den}$ below a threshold of 53 dB(A) already (Environmental noise guidelines for the European Region, 2018). Moreover,

the 5 dB(A) intervals are relatively wide – increasing the number of cars by factor two increments the generated noise by 3 dB(A) only. The relative low errors quantified in Table 3 are therefore still significant. Only a continuous mapping of noise levels would provide respective level of details and should be fostered in the future. Along these noise intervals being critically, using the official noise maps provided access to a very large training data set necessary for such machine learning based research designs. That is, extrapolating the data in order to assess the exposure in larger geographical contexts. The utilized reference data builds upon a diverse dataset from 21 cities. While the training data from these cities encompasses a diverse range of morphological patterns—from dense urban centers to peripheral suburban areas and incorporated village-like settlements—it remains unclear how well the model generalizes to unseen peripheral areas. Here, yet, no data is available for noise emitted from roads with fewer than 3 million vehicle passages per year. Although all of the cities included reported road traffic noise based on the same legal obligation, followed the respective Good-Practice-Guide (WG-AEN, 2007) and utilized certified software packages (Garg and Maji, 2014; Steele, 2001), inconsistencies were observed. So, aiming for consistent reference data, we have carefully selected cities, sharing the same calculation rulesets and post-processing method (Staab et al., 2025). Still, Fig. 3 showed, that specific cities systematically stand out when an else nationwide model is validated against them. This could either be due to a significantly distinct traffic management within these cities, or – most likely – variate implementations of the European mapping standard. The final aggregation of different cities into the weights of one singular model effectively mitigates the local biases of the decentral produced data. In summary, a harmonized and consistent output is facilitated, enabling meaningful comparisons of exposed populations.

Other limitations of the present study refer to the predictor variables. First, relying on traffic road infrastructure (i.e. differentiating functional road types) as proxies for traffic noise emissions is unable to scope local variances. The very fluctuations in traffic flow could be detected using machine learning and camera images for example (Fredianelli et al., 2022; Tian et al., 2019). However, generalizing the traffic flow into six distinct road types significantly reduced the production costs of our noise exposure map. This approach inherits the potential for false positives, false negatives and ill representations where traffic flow splits. Moreover, both the artificially generated noise from electric vehicles (Licitra et al., 2023; Pallas et al., 2016; Steinbach and Altinsoy, 2019) and the fraction of heavy vehicles influence local noise emissions (Federal Ministry of Transport and Digital Infrastructure, 1990), are likely to vary on regional scale. Therefore, further efforts should focus on incorporating industrial POIs, as well as localized vehicle registration statistics and economic and industrial indicators (e.g. from Federal Institute for Research on Building, Urban Affairs, and Spatial Development (BBSR), 2024; German Federal Motor Transport Authority (KBA), 2025). Analog thereto, detailed considerations of road surface materials would enhance the models precision (Ascari et al., 2024; Del Pizzo et al., 2020; Sheng and Wang, 2024; Wrótny et al., 2022; Yang et al., 2025). As well visualized by the large blue proportion of Fig. 1, this involved an extensive feature engineering using various software libraries and geospatial operators. With 82 predictor features, quantitively, a larger feature set was produced compared to prior studies – 4 features when introduced by D. Xie et al. (2011a), up to 29 features utilized by Xu et al. (2022) and 33 features presented to random forest algorithm by Liu et al. (2020). But from a qualitative perspective, only the fundamental parameters such as emission, ground absorbance, urban- and geomorphological sound interactions were preprocessed for the machine learning algorithms. Yet, further features are considerable, as for example the presence of soundproof walls and noise barriers (Reiter et al., 2017; Szopińska et al., 2022). However, this comprehensive approach of curating predictor variables manually undoubtedly required significant time and efforts by domain experts. In this very context, Eicher et al. (2022) emphasized the potential of convolutional neural networks (CNNs) to abstract the feature engineering processes. Though, the RMSE of 8.8 dB(A) using Sentinel-2 data alone (Eicher et al., 2022), stresses that many variances in noise maps do still require auxiliary data to be curated manually. As the computational powers keep increasing (Moore, 1965), machine learning models evolving (Zhu et al., 2017) and the awareness of noise being an environmental burden across the globe (Ögren, 2021), future studies will most probably expand the present path. Both, qualitatively by advancing the input data sources and utilizing stronger models able to interpret interactions within the feature space, as well as spatially (Milojevic-Dupont et al., 2023; Zanaga et al., 2021). Respectively, designing network architectures with hybrid input layers for vectorized auxiliary data such as OSM and building models, as well as earth observation data inputs connected by hidden convolutional layers most importantly is necessary (e.g. Weigand et al., 2023 for mapping green spaces).

In this very context, also the experimental setups configuration may be discussed. Only three hyperparameters were probed. With respect to the *splitrule*, randomized splitting was used without altering further hyperparameters, as for example disabling bagging as in (Geurts et al., 2006). Using a grid search approach, the two other parameters' range was extended around the default values into both directions – without considering alternative tuning strategies such as random search or sequential model-based optimization (Probst et al., 2019). Referring to *mtry* in particular, a too large value potentially allows the model to heavily rely on a few selected predictors only. The predicted map of Experiment 88 (see S3) was patchy compared to the other two suitable models evaluated likely for this reason. Last but not least, the models were tuned towards a high weighted Kappa value. A comparison to other metrics, such as a ROC analysis extend ordinal regression (Waegeman et al., 2006) was outside the scope of this study.

The thorough benchmarking of the SLURM jobs running in parallel provided valuable insights into the mechanics of the random forest architecture. This enables future studies to optimize the allocated resources on their cluster. That said, the findings reveal that model performance does not exhibit a significant correlation with the computational resources invested. This breaks with the conventional assumptions about resource-intensive training and aligns with the narrative of Schwartz et al. (2020), stressing that efficient model configurations can achieve comparable results with both, ecological and economic footprints in mind.

## 7. Conclusion

The gradation from dense urban structures to sparsely populated rural areas, as captured in Fig. 4, underscores the comprehensive nature of our noise prediction model. Supported with multimodal geodata, complex machine learning models are able to predict noise

levels in such varied environments. The resulting exposure estimation of 13.1 million people exposed to road $L_{den}$ above 55 dB(A) highlights a substantial underestimation in official noise mapping. Although, in detail, high fidelity physics-based models are unchallenged in local domains yet the most expensive, it is the rigid generalization of machine learning-based models which allows urban planners and public health officials to compare predicted sound pressure levels of different locations against each other on very large scale only. A practical implementation path could combine the two complementary approaches. In order to benefit from both, the physics-based models may be focused on locations estimated to be critical using our approach at first. Regarding the strong interest in public health and fair living environments not only in cities and along major roads, but also in smaller towns and other modes of transport across the European continent (World Health Organization, 2011), we believe that geostatistical models are one promising pathway to point out highly exposed areas in a cost-efficient manner. Beyond the nationwide scale, pan-European or even global models are reachable.

## Software

The utilized software (and versions) in this study are Gdal (3.2.1), R (4.1.1) using the packages raster (3.5–15), HORIZON (1.2), caret (6.0–94), ranger (0.15.1) and irr (0.84.1), as well as QGis (3.16.5).

## CRediT authorship contribution statement

**Jeroen Staab:** Writing – review & editing, Writing – original draft, Visualization, Validation, Software, Project administration, Methodology, Funding acquisition, Formal analysis, Data curation, Conceptualization. **Matthias Weigand:** Writing – original draft, Visualization, Software, Methodology, Formal analysis. **Arthur Schady:** Writing – original draft, Supervision, Resources, Investigation, Funding acquisition, Formal analysis. **Ariane Droin:** Writing – original draft, Software, Methodology. **Donatella Cea:** Methodology. **Marco Dallavalle:** Writing – review & editing, Validation, Methodology, Funding acquisition. **Nikolaos Nikolaou:** Methodology, Investigation. **Mahyar Valizadeh:** Methodology. **Kathrin Wolf:** Writing – review & editing, Validation, Project administration, Investigation, Funding acquisition, Conceptualization. **Michael Wurm:** Writing – review & editing, Supervision, Resources, Project administration, Investigation, Funding acquisition. **Tobia Lakes:** Writing – review & editing, Supervision, Project administration, Formal analysis, Conceptualization. **Hannes Taubenböck:** Writing – original draft, Supervision, Resources, Project administration, Investigation, Funding acquisition, Conceptualization.

## Declaration of competing interest

The authors declare that they have no known competing financial interests or personal relationships that could have appeared to influence the work reported in this paper.

## Acknowledgments

This study was supported by the DBU (20017/500) and Helmholtz Association's Initiative and Networking Fund (INF): ZT-I-PF-5-42. Reference noise data from roads was obtained from the 2017 Strategic Noise Maps reported under the obligations of the Environmental Noise Directive 2002/49/EC and was downloaded from the central data repository of the European Environment Agency. We acknowledge the data provided by the OpenStreetMap project and its contributors under the terms of the Open Data Commons Open Database License (ODbL) as well as the German Federal Agency for Cartography and Geodesy for providing the LoD1 building model. Moreover, the authors gratefully acknowledge the computational and data resources provided through the joint high-performance data analytics (HPDA) project terrabyte of the German Aerospace Center (DLR) and the Leibniz Supercomputing Center (LRZ) and the excellent support by Peter Friedel. Also, we want to honor our intern Marlene Westecker for her support of this study. Last but not least, we would like to express our sincere gratitude to the editor and the three anonymous reviewers for their insightful comments, constructive feedback, and valuable suggestions, which have significantly improved the quality and clarity of this work. We deeply appreciate their time and effort in reviewing this manuscript.

## Appendix A. Supplementary data

Supplementary data to this article can be found online at https://doi.org/10.1016/j.trd.2025.105063.

## Data availability

The 10 x 10 Meter resolution, nationwide road traffic $L_{den}$ map for Germany 2017 is open accessible via the institute's data repository: https://doi.org/10.15489/5non57bdli63.

## References


Aguilera, I., Foraster, M., Basagaña, X., Corradi, E., Deltell, A., Morelli, X., Phuleria, H.C., Ragettli, M.S., Rivera, M., Thomasson, A., Slama, R., Künzli, N., 2015. Application of land use regression modelling to assess the spatial distribution of road traffic noise in three European cities. J. Eposure Sci. Environ. Epidemiol. 25, 97–105. https://doi.org/10.1038/jes.2014.61.

Ascari, E., Cerchiai, M., Fredianelli, L., Melluso, D., Licitra, G., 2024. Tuning user-defined pavements in CNOSSOS-EU towards reliable estimates of road noise exposure. Transp. Res. Part D: Transp. Environ. 130, 104195. https://doi.org/10.1016/j.trd.2024.104195.

2002/49/EC, 2002. European Noise Directive.

Attenborough, K., 2007. Sound Propagation in the Atmosphere, in: Rossing, T.D. (Ed.), Springer Handbook of Acoustics, Springer Handbooks. Springer, New York, NY, pp. 113–147. https://doi.org/10.1007/978-0-387-30425-0_4.

Aylor, D., 1972. Noise Reduction by Vegetation and Ground. J. Acoust. Soc. Am. 51, 197–205. https://doi.org/10.1121/1.1912830.

Babisch, W., Wolf, K., Petz, M., Heinrich, J., Cyrys, J., Peters, A., 2014. Associations between Traffic Noise, Particulate Air Pollution, Hypertension, and Isolated Systolic Hypertension in Adults: The KORA Study. Environ. Health Perspect. 122, 492–498. https://doi.org/10.1289/ehp.1306981.

Basner, M., Babisch, W., Davis, A., Brink, M., Clark, C., Janssen, S., Stansfeld, S., 2014. Auditory and non-auditory effects of noise on health. Lancet 383, 1325–1332. https://doi.org/10.1016/S0140-6736(13)61613-X.

Beckenbauer, T., 2013. Road Traffic Noise, in: Müller, G., Möser, M. (Eds.), Handbook of Engineering Acoustics. Springer, Berlin, Heidelberg, pp. 367–392. https://doi.org/10.1007/978-3-540-69460-1_15.

Belgiu, M., Drăguţ, L., 2016. Random forest in remote sensing: A review of applications and future directions. ISPRS J. Photogramm. Remote Sens. 114, 24–31. https://doi.org/10.1016/j.isprsjprs.2016.01.011.

Bluhm, G.L., Berglind, N., Nordling, E., Rosenlund, M., 2007. Road traffic noise and hypertension. Occup. Environ. Med. 64, 122–126.

Bolognese, M., Fredianelli, L., Stasi, G., Ascari, E., Crifaci, G., Licitra, G., 2024. Citizens' exposure to predominant noise sources in agglomerations. Noise Mapping 11, 20240007. https://doi.org/10.1515/noise-2024-0007.

Breiman, L., 2001. Random forests. Machine learning 45, 5–32. https://doi.org/10.1023/a:1010933404324.

Brumm, H. (Ed.), 2013. Animal Communication and Noise, Animal Signals and Communication. Springer Berlin Heidelberg, Berlin, Heidelberg. https://doi.org/10.1007/978-3-642-41494-7.

Bundesanstalt für Straßenwesen, 2006. Vorläufige Berechnungsmethode für den Umgebungslärm an Straßen – VBUS (Fachveröffentlichung). Bundesanstalt für Straßenwesen.

Chang, T.-Y., Liang, C.-H., Wu, C.-F., Chang, L.-T., 2019. Application of land-use regression models to estimate sound pressure levels and frequency components of road traffic noise in Taichung, Taiwan. Environment International 131, 104959. https://doi.org/10.1016/j.envint.2019.104959.

Cohen, J., 1968. Weighted kappa: Nominal scale agreement provision for scaled disagreement or partial credit. Psychol. Bull. 70, 213–220. https://doi.org/10.1037/h0026256.

De Coensel, B., De Muer, T., Yperman, I., Botteldooren, D., 2005. The influence of traffic flow dynamics on urban soundscapes. Appl. Acoust. 66, 175–194. https://doi.org/10.1016/j.apacoust.2004.07.012.

Del Pizzo, L.G., Teti, L., Moro, A., Bianco, F., Fredianelli, L., Licitra, G., 2020. Influence of texture on tyre road noise spectra in rubberized pavements. Appl. Acoust. 159, 107080. https://doi.org/10.1016/j.apacoust.2019.107080.

Dozier, J., Frew, J., 1990. Rapid calculation of terrain parameters for radiation modeling from digital elevation data. IEEE Trans. Geosci. Remote Sens. 28, 963–969. https://doi.org/10.1109/36.58986.

Dratva, J., Phuleria, H.C., Foraster, M., Gaspoz, J.-M., Keidel, D., Künzli, N., Liu, L.-J.-S., Pons, M., Zemp, E., Gerbase, M.W., Schindler, C., 2012. Transportation Noise and Blood Pressure in a Population-Based Sample of Adults. Environ. Health Perspect. 120, 50–55. https://doi.org/10.1289/ehp.1103448.

Eicher, L., Mommert, M., Borth, D., 2022. Traffic Noise Estimation from Satellite Imagery with Deep Learning, in: IGARSS 2022 - 2022 IEEE International Geoscience and Remote Sensing Symposium. Presented at the IGARSS 2022 - 2022 IEEE International Geoscience and Remote Sensing Symposium, IEEE, Kuala Lumpur, Malaysia, pp. 5937–5940. https://doi.org/10.1109/IGARSS46834.2022.9883463.

Environmental noise guidelines for the European Region, 2018. . World Health Organization, Regional Office for Europe, Copenhagen, Denmark.

Erickson, L.C., Newman, R.S., 2017. Influences of Background Noise on Infants and Children. Curr. Dir. Psychol. Sci. 26, 451–457. https://doi.org/10.1177/0963721417709087.

European Commission, 2021. Assessment of potential health benefits of noise abatement measures in the EU: Phenomena project. Publications Office, LU.

European Environment Agency, 2020a. Environmental noise in Europe - 2020. Publications Office, LU.

European Environment Agency, 2020b. Urban Atlas 2018 — Copernicus Land Monitoring Service.

Evans, G.W., Hygge, S., Bullinger, M., 1995. Chronic noise and psychological stress. Psychol. Sci. 6, 333–338.

Federal Institute for Research on Building, Urban Affairs, and Spatial Development (BBSR), 2024. Ongoing Spatial Observation by the BBSR - INKAR, Edition 03/2024.

Federal Ministry of Transport and Digital Infrastructure, 1990. Guidelines for Noise Protection on Roads (RLS-90). Köln 1, 07–08.

Francis, C.D., Kleist, N.J., Ortega, C.P., Cruz, A., 2012. Noise pollution alters ecological services: enhanced pollination and disrupted seed dispersal. Proc. R. Soc. B Biol. Sci. 279, 2727–2735. https://doi.org/10.1098/rspb.2012.0230.

Fredianelli, L., Carpita, S., Bernardini, M., Del Pizzo, L.G., Brocchi, F., Bianco, F., Licitra, G., 2022. Traffic Flow Detection Using Camera Images and Machine Learning Methods in ITS for Noise Map and Action Plan Optimization. Sensors 22, 1929. https://doi.org/10.3390/s22051929.

Gamer, M., Lemon, J., Singh <puspendra.pusp22@gmail.com>, I.F.P., 2019. irr: Various Coefficients of Interrater Reliability and Agreement.

Garg, N., Maji, S., 2014. A critical review of principal traffic noise models: Strategies and implications. Environ. Impact Assess. Rev. 46, 68–81. https://doi.org/10.1016/j.eiar.2014.02.001.

German Federal Motor Transport Authority (KBA), 2025. Passenger cars with electric drive – Inventory as of January 1, 2025 by region (dashboard) [WWW Document]. URL https://experience.arcgis.com/experience/85fe6a72369a4700878c72bb9da8dfa6 (accessed 6.2.25).

Geurts, P., Ernst, D., Wehenkel, L., 2006. Extremely randomized trees. Mach. Learn. 63, 3–42. https://doi.org/10.1007/s10994-006-6226-1.

Gharehchahi, E., Hashemi, H., Yunesian, M., Samaei, M., Azhdarpoor, A., Oliaei, M., Hoseini, M., 2024. Geospatial analysis for environmental noise mapping: A land use regression approach in a metropolitan city. Environ. Res. 257, 119375. https://doi.org/10.1016/j.envres.2024.119375.

Gorelick, N., Hancher, M., Dixon, M., Ilyushchenko, S., Thau, D., Moore, R., 2017. Google Earth Engine: Planetary-scale geospatial analysis for everyone. Remote Sens. Environ. 202, 18–27. https://doi.org/10.1016/j.rse.2017.06.031.

Goudreau, S., Plante, C., Fournier, M., Brand, A., Roche, Y., Smargiassi, A., 2014. Estimation of Spatial Variations in Urban Noise Levels with a Land Use Regression Model. EP 3, p48. https://doi.org/10.5539/ep.v3n4p48.

Hahad, O., Kröller-Schön, S., Daiber, A., Münzel, T., 2019. The Cardiovascular Effects of Noise. Deutsches Ärzteblatt international. https://doi.org/10.3238/arztebl.2019.0245.

Harouvi, O., Ben-Elia, E., Factor, R., de Hoogh, K., Kloog, I., 2018. Noise estimation model development using high-resolution transportation and land use regression. J. Expo. Sci. Environ. Epidemiol. 28, 559–567. https://doi.org/10.1038/s41370-018-0035-z.

He, H., Garcia, E.A., 2009. Learning from Imbalanced Data. IEEE Trans. Knowl. Data Eng. 21, 1263–1284. https://doi.org/10.1109/TKDE.2008.239.

Helbich, M., Hagenauer, J., Burov, A., Dzhambov, A.M., 2025. Traffic noise assessment in urban Bulgaria using explainable machine learning. Sustain. Cities Soc. 120, 106169. https://doi.org/10.1016/j.scs.2025.106169.

Heutschi, K., 1995. A simple method to evaluate the increase of traffic noise emission level due to buildings, for a long straight street. Appl. Acoust. 44, 259–274.

Huang, S., Tang, L., Hupy, J.P., Wang, Y., Shao, G., 2021. A commentary review on the use of normalized difference vegetation index (NDVI) in the era of popular remote sensing. J. For. Res. 32, 1–6. https://doi.org/10.1007/s11676-020-01155-1.

Karges, N., Staab, J., Rauh, J., Wegmann, M., Taubenböck, H., 2022. Soundscapes on edge - The real-time machine learning approach for measuring Soundscapes on resource-constrained devices. Proceedings of the 24th International Congress on Acoustics. Presented at the 24th International Congress on Acoustics.
Karges, N., Staab, J., Taubenböck, H., Rauh, J., 2025. Urban contexts: A geospatial approach to identifying in-situ measurement sites for urban acoustic environments. J. Environ. Manage. 389, 125901. https://doi.org/10.1016/j.jenvman.2025.125901.
Khan, J., Ketzel, M., Jensen, S.S., Gulliver, J., Thysell, E., Hertel, O., 2021. Comparison of Road Traffic Noise prediction models: CNOSSOS-EU, Nord2000 and TRANEX. Environ. Pollut. 270, 116240. https://doi.org/10.1016/j.envpol.2020.116240.
Khomenko, S., Cirach, M., Barrera-Gómez, J., Pereira-Barboza, E., Iungman, T., Mueller, N., Foraster, M., Tonne, C., Thondoo, M., Jephcote, C., Gulliver, J., Woodcock, J., Nieuwenhuijsen, M., 2022. Impact of road traffic noise on annoyance and preventable mortality in European cities: A health impact assessment. Environ. Int. 162, 107160. https://doi.org/10.1016/j.envint.2022.107160.
Kim, P., Ryu, H., Jeon, J.-J., Chang, S.I., 2021. Statistical Road-Traffic Noise Mapping Based on Elementary Urban Forms in Two Cities of South Korea. Sustainability 13, 2365. https://doi.org/10.3390/su13042365.
Kuhn, M., 2008. Building Predictive Models in R Using the caret Package. J. Stat. Softw. 28, 1–26.
Kukulski, B., Wszołek, T., 2022. Development of parameter-based criteria for applying adjustment for highly impulsive sound sources. Appl. Acoust. 185, 108375. https://doi.org/10.1016/j.apacoust.2021.108375.
Kumar, S., Garg, N., 2025. Integrated land use regression (iLUR) model with road traffic characteristics for environmental noise prediction and mapping in urban regions with heterogenous traffic conditions. Appl. Acoust. 239, 110830. https://doi.org/10.1016/j.apacoust.2025.110830.
Lavandier, C., Regragui, M., Dedieu, R., Royer, C., Can, A., 2022. Influence of road traffic noise peaks on reading task performance and disturbance in a laboratory context. Acta Acust. 6, 3. https://doi.org/10.1051/aacus/2021057.
Lee, C.A., Gasster, S.D., Plaza, A., Chang, C.-I., Huang, B., 2011. Recent Developments in High Performance Computing for Remote Sensing: A Review. IEEE J. Sel. Top. Appl. Earth Observations Remote Sensing 4, 508–527. https://doi.org/10.1109/JSTARS.2011.2162643.
Lee, P.J., Park, S.H., Jeong, J.H., Choung, T., Kim, K.Y., 2019. Association between transportation noise and blood pressure in adults living in multi-storey residential buildings. Environ. Int. 132, 105101. https://doi.org/10.1016/j.envint.2019.105101.
Licitra, G., Bernardini, M., Moreno, R., Bianco, F., Fredianelli, L., 2023. CNOSSOS-EU coefficients for electric vehicle noise emission. Appl. Acoust. 211, 109511. https://doi.org/10.1016/j.apacoust.2023.109511.
Licitra, G., Bolognese, M., Chiari, C., Carpita, S., Fredianelli, L., 2022. Noise Source Predominance Map: a new representation for strategic noise maps. Noise Mapping 9, 269–279. https://doi.org/10.1515/noise-2022-0163.
Liu, Y., Goudreau, S., Oiamo, T., Rainham, D., Hatzopoulou, M., Chen, H., Davies, H., Tremblay, M., Johnson, J., Bockstael, A., Leroux, T., Smargiassi, A., 2020. Comparison of land use regression and random forests models on estimating noise levels in five Canadian cities. Environ. Pollut. 256, 113367. https://doi.org/10.1016/j.envpol.2019.113367.
Margaritis, E., Kang, J., 2017. Relationship between green space-related morphology and noise pollution. Ecol. Ind. 72, 921–933. https://doi.org/10.1016/j.ecolind.2016.09.032.
Margaritis, E., Kang, J., Filipan, K., Botteldooren, D., 2018. The influence of vegetation and surrounding traffic noise parameters on the sound environment of urban parks. Appl. Geogr. 94, 199–212. https://doi.org/10.1016/j.apgeog.2018.02.017.
Marquis-Favre, C., Braga, R., Gourdon, E., Combe, C., Gille, L.-A., Ribeiro, C., Mietlicki, F., 2023. Estimation of psychoacoustic and noise indices from the sound pressure level of transportation noise sources: Investigation of their potential benefit to the prediction of long-term noise annoyance. Appl. Acoust. 211, 109560. https://doi.org/10.1016/j.apacoust.2023.109560.
Miedema, H.M., Oudshoorn, C.G., 2001. Annoyance from transportation noise: relationships with exposure metrics DNL and DENL and their confidence intervals. Environ. Health Perspect. 109, 409–416. https://doi.org/10.1289/ehp.01109409.
Milojevic-Dupont, N., Wagner, F., Nachtigall, F., Hu, J., Brüser, G.B., Zumwald, M., Biljecki, F., Heeren, N., Kaack, L.H., Pichler, P.-P., Creutzig, F., 2023. EUBUCCO v0.1: European building stock characteristics in a common and open database for 200+ million individual buildings. Sci. Data 10, 147. https://doi.org/10.1038/s41597-023-02040-2.
Moore, G.E., 1965. Cramming more components onto integrated circuits. Electronics 38, 114–117.
Müller, J., Bartolomaeus, W., 2015. Comparison between German Road Traffic Noise Calculation Method and new Common Noise Assessment Methods.
Muzet, A., 2007. Environmental noise, sleep and health. Sleep Med. Rev. 11, 135–142. https://doi.org/10.1016/j.smrv.2006.09.001.
Niedermayer, F., Rospleszcz, S., Matthiessen, C., Hoffmann, B., Stoecklein, S., Haueise, T., Norajitra, T., Schlett, C.L., Nattenmüller, J., Bamberg, F., Machann, J., Günther, M., Hirsch, J., Nagrani, R., Völzke, H., Meinke-Franze, C., Hosten, N., Nonnenmacher, T., Budai, B.K., Palm, V., Katzke, V., Greiser, K.H., Schulz-Menger, J., Niendorf, T., Endemann, B., Pischon, T., Staab, J., Dallavalle, M., Schneider, A., Wolf, K., Peters, A., 2025. Associations of road traffic noise with adipose tissue depots and hepatic fat content – Results from the German National Cohort (NAKO). Environ. Int. 201, 109566. https://doi.org/10.1016/j.envint.2025.109566.
Ögren, M., 2021. Estimating noise exposure for burden of disease calculations in country-sized areas. Presented at the ICBEN Congresses on Noise as a Public Health Problem, Stockholm.
Öhström, E., Rylander, R., 1990. Sleep disturbance by road traffic noise—A laboratory study on number of noise events. J. Sound Vib. 143, 93–101. https://doi.org/10.1016/0022-460X(90)90570-P.
Ostashev, V.E., Wilson, D.K., 2015. Acoustics in moving inhomogeneous media. CRC Press.
Pallas, M.-A., Berengier, M., Chatagnon, R., Czuka, M., Conter, M., Muirhead, M., 2016. Towards a model for electric vehicle noise emission in the European prediction method CNOSSOS-EU. Appl. Acoust. 113, 89–101.
Pan, S.J., Yang, Q., 2010. A Survey on Transfer Learning. IEEE Trans. Knowl. Data Eng. 22, 1345–1359. https://doi.org/10.1109/TKDE.2009.191.
Pascale, A., Fernandes, P., Macedo, E., Guarnaccia, C., Coelho, M.C., 2024. Mapping noise and pollutant emissions hotspots: Driving behavior and vehicle features based-analysis. Transp. Res. Part D: Transp. Environ. 136, 104466. https://doi.org/10.1016/j.trd.2024.104466.
Peters, A., Peters, A., Greiser, K.H., Göttlicher, S., Ahrens, W., Albrecht, M., Bamberg, F., Bärnighausen, T., Becher, H., Berger, K., Beule, A., Boeing, H., Bohn, B., Bohnert, K., Braun, B., Brenner, H., Bülow, R., Castell, S., Damms-Machado, A., Dörr, M., Ebert, N., Ecker, M., Emmel, C., Fischer, B., Franzke, C.-W., Gastell, S., Giani, G., Günther, M., Günther, K., Günther, K.-P., Haerting, J., Haug, U., Heid, I.M., Heier, M., Heinemeyer, D., Hendel, T., Herbolsheimer, F., Hirsch, J., Hoffmann, W., Holleczek, B., Hölling, H., Hörlein, A., Jöckel, K.-H., Kaaks, R., Karch, A., Karrasch, S., Kartschmit, N., Kauczor, H.-U., Keil, T., Kemmling, Y., Klee, B., Klüppelholz, B., Kluttig, A., Kofink, L., Köttgen, A., Kraft, D., Krause, G., Kretz, L., Krist, L., Kühnisch, J., Kuß, O., Legath, N., Lehnich, A.-T., Leitzmann, M., Lieb, W., Linseisen, J., Loeffler, M., Macdonald, A., Maier-Hein, K.H., Mangold, N., Meinke-Franze, C., Meisinger, C., Melzer, J., Mergarten, B., Michels, K.B., Mikolajczyk, R., Moebus, S., Mueller, U., Nauck, M., Niendorf, T., Nikolaou, K., Obi, N., Ostrzinski, S., Panreck, L., Pigeot, I., Pischon, T., Pschibul-Thamm, I., Rathmann, W., Reineke, A., Roloff, S., Rujescu, D., Rupf, S., Sander, O., Schikowski, T., Schipf, S., Schirmacher, P., Schlett, C.L., Schmidt, B., Schmidt, G., Schmidt, M., Schöne, G., Schulz, H., Schulze, M.B., Schweig, A., Sedlmeier, A.M., Selder, S., Six-Merker, J., Sowade, R., Stang, A., Stegle, O., Steindorf, K., Stübs, G., Swart, E., Teismann, H., Thiele, I., Thierry, S., Ueffing, M., Völzke, H., Waniek, S., Weber, A., Werner, N., Wichmann, H.-E., Willich, S.N., Wirkner, K., Wolf, K., Wolff, R., Zeeb, H., Zinkhan, M., Zschocke, J., German National Cohort (NAKO) Consortium, 2022. Framework and baseline examination of the German National Cohort (NAKO). Eur J Epidemiol 37, 1107–1124. https://doi.org/10.1007/s10654-022-00890-5.
Petri, D., Licitra, G., Vigotti, M.A., Fredianelli, L., 2021. Effects of Exposure to Road, Railway, Airport and Recreational Noise on Blood Pressure and Hypertension. Int. J. Environ. Res. Public Health 18, 9145. https://doi.org/10.3390/ijerph18179145.
Piercy, J.E., Embleton, T.F.W., Sutherland, L.C., 1977. Review of noise propagation in the atmosphere. J. Acoust. Soc. Am. 61, 1403–1418. https://doi.org/10.1121/1.381455.
Pitchika, A., Hampel, R., Wolf, K., Kraus, U., Cyrys, J., Babisch, W., Peters, A., Schneider, A., 2017. Long-term associations of modeled and self-reported measures of exposure to air pollution and noise at residence on prevalent hypertension and blood pressure. Science of The Total Environment 593–594, 337–346. https://doi.org/10.1016/j.scitotenv.2017.03.156.
Probst, P., Wright, M.N., Boulesteix, A.-L., 2019. Hyperparameters and tuning strategies for random forest. WIREs Data Min. Knowl. Discovery 9, e1301.

R Core Team, 2023. R: A Language and Environment for Statistical Computing. R Foundation for Statistical Computing, Vienna, Austria.
Raess, M., Brentani, V.M., A., Flückiger, B., Ledebur de Antas de Campos, B., Fink, G., Röösli, M., 2022. Association between community noise and children's cognitive and behavioral development: A prospective cohort study. Environ. Int. 158, 106961. https://doi.org/10.1016/j.envint.2021.106961.
Ragettli, M.S., Goudreau, S., Plante, C., Fournier, M., Hatzopoulou, M., Perron, S., Smargiassi, A., 2016. Statistical modeling of the spatial variability of environmental noise levels in Montreal, Canada, using noise measurements and land use characteristics. J. Expo. Sci. Environ. Epidemiol. 26, 597–605. https://doi.org/10.1038/jes.2015.82.
Rajala, V., Hongisto, V., 2020. Annoyance penalty of impulsive noise – The effect of impulse onset. Build. Environ. 168, 106539. https://doi.org/10.1016/j.buildenv.2019.106539.
Reethof, G., 1973. Effect of Plantings on Radiation of Highway Noise. J. Air Pollut. Control Assoc. 23, 185–189. https://doi.org/10.1080/00022470.1973.10469763.
Reiter, P., Wehr, R., Ziegelwanger, H., 2017. Simulation and measurement of noise barrier sound-reflection properties. Appl. Acoust. 123, 133–142. https://doi.org/10.1016/j.apacoust.2017.03.007.
Riedel, N., Scheiner, J., Müller, G., Köckler, H., 2014. Assessing the relationship between objective and subjective indicators of residential exposure to road traffic noise in the context of environmental justice. J. Environ. Plan. Manag. 57, 1398–1421. https://doi.org/10.1080/09640568.2013.808610.
Roberts, D.R., Bahn, V., Ciuti, S., Boyce, M.S., Elith, J., Guillera-Arroita, G., Hauenstein, S., Lahoz-Monfort, J.J., Schröder, B., Thuiller, W., Warton, D.I., Wintle, B.A., Hartig, F., Dormann, C.F., 2017. Cross-validation strategies for data with temporal, spatial, hierarchical, or phylogenetic structure. Ecography 40, 913–929. https://doi.org/10.1111/ecog.02881.
Rossi, L., Prato, A., Lesina, L., Schiavi, A., 2018. Effects of low-frequency noise on human cognitive performances in laboratory. Build. Acoust. 25, 17–33. https://doi.org/10.1177/1351010X18756800.
Schwartz, R., Dodge, J., Smith, N.A., Etzioni, O., 2020. Green AI. Commun. ACM 63, 54–63. https://doi.org/10.1145/3381831.
Sharma, J., Jetschny, S., Maza, M.S., Guardia, N.B., Peris, E., Esteve, J.F., Belaid, M.B., 2024. Deep Neural Networks for Comprehensive Environmental Noise Estimation in European Cities. In: 2024 International Conference on Machine Learning and Applications (ICMLA). Presented at the 2024 International Conference on Machine Learning and Applications (ICMLA), pp. 71–78. https://doi.org/10.1109/ICMLA61862.2024.00016.
Sheng, W., Wang, Y., 2024. Traffic noise mitigation through texture-induced quiet pavement: Analytical modeling and field test. Transp. Res. Part D: Transp. Environ. 137, 104485. https://doi.org/10.1016/j.trd.2024.104485.
Sieber, C., Ragettli, M.S., Brink, M., Toyib, O., Baatjies, R., Saucy, A., Probst-Hensch, N., Dalvie, M.A., Röösli, M., 2017. Land Use Regression Modeling of Outdoor Noise Exposure in Informal Settlements in Western Cape, South Africa. Int. J. Environ. Res. Public Health 14, 1262. https://doi.org/10.3390/ijerph14101262.
Silva, L.T., Fonseca, F., Rodrigues, D., Campos, A., 2018. Assessing the influence of urban geometry on noise propagation by using the sky view factor. J. Environ. Plan. Manag. 61, 535–552. https://doi.org/10.1080/09640568.2017.1319804.
Staab, J., Droin, A., Weigand, M., Dallavalle, M., Wolf, K., Schady, A., Lakes, T., Wurm, M., Taubenböck, H., 2025. Pixels, chisels and contours - technical variations in European road traffic noise exposure maps. J. Environ. Manage. 385, 125475. https://doi.org/10.1016/j.jenvman.2025.125475.
Staab, J., Schady, A., Weigand, M., Lakes, T., Taubenböck, H., 2022. Predicting traffic noise using land-use regression—a scalable approach. J. Eposure Sci. Environ. Epidemiol. 32, 232–243. https://doi.org/10.1038/s41370-021-00355-z.
Staab, J., Stark, T., Wurm, M., Wolf, K., Dallavalle, M., Schady, A., Lakes, T., Taubenböck, H., 2023. Using CNNs on Sentinel-2 data for road traffic noise modelling, in: 2023 Joint Urban Remote Sensing Event (JURSE). Presented at the 2023 Joint Urban Remote Sensing Event (JURSE), pp. 1–4. https://doi.org/10.1109/JURSE57346.2023.10144160.
Stansfeld, S.A., 2003. Noise pollution: non-auditory effects on health. Br. Med. Bull. 68, 243–257. https://doi.org/10.1093/bmb/ldg033.
Steele, C., 2001. A critical review of some traffic noise prediction models. Appl. Acoust. 62, 271–287. https://doi.org/10.1016/S0003-682X(00)00030-X.
Steinbach, L., Altinsoy, M.E., 2019. Prediction of annoyance evaluations of electric vehicle noise by using artificial neural networks. Appl. Acoust. 145, 149–158. https://doi.org/10.1016/j.apacoust.2018.09.024.
Suits, D.B., 1957. Use of Dummy Variables in Regression Equations. J. Am. Stat. Assoc. 52, 548–551. https://doi.org/10.1080/01621459.1957.10501412.
Szopińska, K., Balawejder, M., Warchoł, A., 2022. National legal regulations and location of noise barriers along the Polish highway. Transp. Res. Part D: Transp. Environ. 109, 103359. https://doi.org/10.1016/j.trd.2022.103359.
Tang, M., Li, X., 2024. Growing disparities in transportation noise exposure across major US cities over time. Transp. Res. Part D: Transp. Environ. 136, 104430. https://doi.org/10.1016/j.trd.2024.104430.
Taubenböck, H., Standfuß, I., Wurm, M., Krehl, A., Siedentop, S., 2017. Measuring morphological polycentricity - A comparative analysis of urban mass concentrations using remote sensing data. Comput. Environ. Urban Syst. 64, 42–56. https://doi.org/10.1016/j.compenvurbsys.2017.01.005.
Taubenböck, H., Weigand, M., Esch, T., Staab, J., Wurm, M., Mast, J., Dech, S., 2019. A new ranking of the world's largest cities—Do administrative units obscure morphological realities? Remote Sens. Environ. 232, 111353. https://doi.org/10.1016/j.rse.2019.111353.
Thorsson, P.J., Ögren, M., 2005. Macroscopic modeling of urban traffic noise – influence of absorption and vehicle flow distribution. Appl. Acoust. 66, 195–209. https://doi.org/10.1016/j.apacoust.2004.07.013.
Tian, S., Yu, H., Yang, Z., Jing, X., Zhang, Z., Shi, M., Wang, Y., 2019. An Improved Target Detection and Traffic Parameter Calculation Method Based on YOLO with a Monocular Camera, in: CICTP 2019. Presented at the 19th COTA International Conference of Transportation Professionals, American Society of Civil Engineers, Nanjing, China, pp. 5696–5708. https://doi.org/10.1061/9780784482292.490.
Van doninck, J., 2018. Horizon Search Algorithm. 'horizon' package documentation.
van Kempen, E., Babisch, W., 2012. The quantitative relationship between road traffic noise and hypertension: a meta-analysis. J. Hypertens. 30, 1075–1086. https://doi.org/10.1097/HJH.0b013e328352ac54.
Virjonen, P., Hongisto, V., Radun, J., 2019. Annoyance penalty of periodically amplitude-modulated wide-band sound. J. Acoust. Soc. Am. 146, 4159–4170. https://doi.org/10.1121/1.5133478.
Waegeman, W., De Baets, B., Boullart, L., 2006. A comparison of different ROC measures for ordinal regression. Proceedings of the CML 2006 Workshop on ROC Analysis in Machine Learning.
Wang, B., Kang, J., 2011. Effects of urban morphology on the traffic noise distribution through noise mapping: A comparative study between UK and China. Appl. Acoust. 72, 556–568. https://doi.org/10.1016/j.apacoust.2011.01.011.
Wang, J., Jin, J., Chen, Y., Shen, P., Sun, Y., Jiang, Z., Guo, X., Wang, H., Li, G., Shui, L., Huang, J., 2025. High spatial resolution environmental noise assessment and its associations with risks of cardiovascular diseases based on digital healthcare data in China. Environ. Int. 109408. https://doi.org/10.1016/j.envint.2025.109408.
Waye, K.P., van Kempen, E., 2021. Non-auditory effects of noise: an overview of the state of the science of the 2017-2020 period. In: Presented at the 3th ICBEN Congress on Noise as a Public Health Problem, p. 35.
Weigand, M., Staab, J., Wurm, M., Taubenböck, H., 2020. Spatial and semantic effects of LUCAS samples on fully automated land use/land cover classification in high-resolution Sentinel-2 data. Int. J. Appl. Earth Obs. Geoinf. 88, 102065. https://doi.org/10.1016/j.jag.2020.102065.
Weigand, M., Wurm, M., Droin, A., Stark, T., Staab, J., Rauh, J., Taubenböck, H., 2023. Are public green spaces distributed fairly? A nationwide analysis based on remote sensing, OpenStreetMap and census data. Geocarto Int. 1–36. https://doi.org/10.1080/10106049.2023.2286305.
WG-AEN, 2007. Good Practice Guide for Strategic Noise Mapping and the Production of Associated Data on Noise Exposure, 2nd ed.
Wolf, K., Dallavalle, M., Niedermayer, F., Bolte, G., Lakes, T., Schikowski, T., Greiser, K.H., Schwettmann, L., Westerman, R., Nikolaou, N., Staab, J., Wolff, R., Stübs, G., Rach, S., Schneider, A., Peters, A., Hoffmann, B., 2025. Environmental exposure assessment in the German National Cohort (NAKO). Environ. Res. 273, 121259. https://doi.org/10.1016/j.envres.2025.121259.
World Health Organization (Ed.), 2011. Burden of disease from environmental noise: quantification of healthy life years lost in Europe. World Health Organization, Regional Office for Europe, Copenhagen.
Wright, M.N., Ziegler, A., 2017. ranger : A Fast Implementation of Random Forests for High Dimensional Data in C++ and R. J. Stat. Soft. 77. https://doi.org/10.18637/jss.v077.i01.

Wrótny, M., Bohatkiewicz, J., Bohatkiewicz-Czaicka, J., 2022. Influence of using low-noise pavements on residents' perception of road noise protection. Transp. Res. Part D: Transp. Environ. 113, 103531. https://doi.org/10.1016/j.trd.2022.103531.

Xie, D., Liu, Y., Chen, J., 2011a. Mapping Urban Environmental Noise: A Land Use Regression Method. Environ. Sci. Technol. 45, 7358–7364. https://doi.org/10.1021/es200785x.

Xie, H., Kang, J., Tompsett, R., 2011b. The impacts of environmental noise on the academic achievements of secondary school students in Greater London. Appl. Acoust. 72, 551–555. https://doi.org/10.1016/j.apacoust.2010.10.013.

Xu, H., Zhang, L., Chang, H., Han, J., Wu, D., Gong, X., Fu, M., 2023. Measuring the route topography impact on real driving emissions based on neural network models. Environ. Res. 231, 116072. https://doi.org/10.1016/j.envres.2023.116072.

Xu, X., Ge, Y., Wang, W., Lei, X., Kan, H., Cai, J., 2022. Application of land use regression to map environmental noise in Shanghai. China. Environment International 161, 107111. https://doi.org/10.1016/j.envint.2022.107111.

Yadav, A., Mandhani, J., Parida, M., Kumar, B., 2022. Modelling of traffic noise in the vicinity of urban road intersections. Transp. Res. Part D: Transp. Environ. 112, 103474. https://doi.org/10.1016/j.trd.2022.103474.

Yadav, A., Parida, M., Choudhary, P., Kumar, B., 2025. Modelling traffic noise-induced annoyance at intersections and its association with psychological health. Transp. Res. Part D: Transp. Environ. 139, 104568. https://doi.org/10.1016/j.trd.2024.104568.

Yang, B., Yuan, M., Weng, Z., Li, D., Leng, Z., 2025. Acoustic aging of low-noise pavements in Hong Kong: Regression modelling and mechanism investigation. Transp. Res. Part D: Transp. Environ. 144, 104793. https://doi.org/10.1016/j.trd.2025.104793.

Yu, T., Zhu, H., 2020. Hyper-Parameter Optimization: A Review of Algorithms and Applications. https://doi.org/10.48550/arXiv.2003.05689.

Zanaga, D., Van De Kerchove, R., De Keersmaecker, W., Souverijns, N., Brockmann, C., Quast, R., Wevers, J., Grosu, A., Paccini, A., Vergnaud, S., Cartus, O., Santoro, M., Fritz, S., Georgieva, I., Lesiv, M., Carter, S., Herold, M., Li, L., Tsendbazar, N.-E., Ramoino, F., Arino, O., 2021. ESA WorldCover 10 m 2020 v100. https://doi.org/10.5281/ZENODO.5571936.

Zhu, X.X., Tuia, D., Mou, L., Xia, G.-S., Zhang, L., Xu, F., Fraundorfer, F., 2017. Deep Learning in Remote Sensing: A Comprehensive Review and List of Resources. IEEE Geosci. Remote Sens. Mag. 5, 8–36. https://doi.org/10.1109/MGRS.2017.2762307.